RSC Advances

PAPER

View Article Online
View Journal | View Issue



Cite this: *RSC Adv.*, 2015, **5**, 100281

# New acetylacetone-polymer modified nanoparticles as magnetically separable complexing agents†

I. Misztalewska,[a] A. Z. Wilczewska,*[a] O. Wojtasik,[a] K. H. Markiewicz,[a] P. Kuchlewski[a] and A. M. Majcher[b]

Received 29th September 2015
Accepted 13th November 2015

DOI: 10.1039/c5ra20137c

www.rsc.org/advances

In this paper, we present two methods of synthesis of new bifunctional polymeric nanohybrids and their full characterization. These nanohybrids consist of a magnetic nanoparticle core and polymeric shell which possess the ability to complex metal ions and organic compounds. Synthesized materials exhibit superparamagnetic properties and can thus be easily separated from complex mixtures by using an external magnetic field (facile separation, purification and recyclability). Herein, the syntheses of three bifunctional monomers are presented. Each of them was used to prepare the homopolymeric shell and two types of copolymeric shells (using styrene as a comonomer) around the magnetite nanoparticles. A surface initiated RAFT/MADIX polymerization technique was employed to prepare polymeric shells. Afterwards, post-modification of azide functionalized polymeric shells using the Huisgen "click" reaction was performed. Finally, twelve types of nanohybrids were prepared and their physicochemical properties were investigated. Additionally, the ability of nanohybrids to complex lanthanides and spectroscopic properties of obtained materials were studied.

## 1. Introduction

β-Diketones represent one of the oldest classes of versatile chelating ligands forming very stable chelate complexes with various metal ions.[1] Plenty of studies have been done on these chelating reagents, especially in the field of solvent extraction of metal ions.[2] In recent decades, complexes of lanthanide (europium,[3] terbium) ions and β-diketones have attracted much attention because of their spectroscopic properties. They are widely used as *e.g.* light-converting optical materials, light-emitting diodes, luminescent probes, *etc.*[4] One of the best-known compounds, which belongs to this group, is acetylacetone. Acetylacetone, as such, is used as a chelating agent in *e.g.* nanoparticles synthesis ($BaTiO_3$),[5] sol–gel synthesis method ($MgAl_2O_4$ powders),[6] Michael polyaddition reaction[7] and spray pyrolysis solutions (preparation of indium, tin oxide films).[8] It is also used as a metal-complexing agent in formation of a variety of catalysts, *e.g.* iron, cobalt or nickel complexes in oxidation reactions.[9] Acetylacetonate metal organic complexes show nucleophilicity, electrophilicity, ability of oxidation–reduction, and selectivity in some chemical reactions. This makes them an ideal homogeneous catalysts for organic synthetic chemistry.[10] Furthermore, anticancer and insulin mimetic activity of vanadyl acetylacetonate complex were examined.[11] However, due to their bad solubility in water and good solubility in organic solvents, acetylacetonate metal organic complexes are difficult to recover from the organic solution by water wash method. Additionally, these complexes are usually thermally unstable because of their low decomposition temperatures.[12] These problems could be solved by anchoring ligands/complexes on a solid phase, for example on magnetic nanoparticles surface (MNP). Thin and homogenous polymer shells with acetylacetonate moiety around MNP can be obtain by surface initiated RAFT/MADIX polymerization technique.

RAFT/MADIX (Reversible Addition–Fragmentation chain Transfer/Macromolecular Design *via* Interchange of Xanthates) technique is a type of controlled radical polymerization which utilizes dithiocarbonates (xanthates) to mediate polymerization by a reversible chain transfer process. It can be realized by simple introduction of a small amount of dithiocarbonate to a conventional free-radical system (monomer + initiator). This polymerization method provides control over growth, dispersity, composition and architecture of polymers.[13] Therefore, a variety of polymeric layers with well-designed and well-defined properties can be obtained. Another advantage of RAFT/MADIX polymerization is a great tolerance of dithiocarbonates (DTC) towards most of the functional groups present in monomer.[14]

In this paper, a "grafting from" approach was applied to introduce DTC on the surface of magnetic nanoparticles (MNP).

[a]*University of Bialystok, Insitute of Chemistry, K. Ciolkowskiego 1K, 15-245 Bialystok, Poland. E-mail: agawilcz@uwb.edu.pl*

[b]*Jagiellonian University, Faculty of Physics, Astronomy and Applied Computer Science, Prof. S. Lojasiewicza 11, 30-348 Cracow, Poland*

† Electronic supplementary information (ESI) available: Additional experimental data, IR, UV-Vis, luminescence and NMR spectras, TGA/DTG curves, SEM/EDX measurements. See DOI: 10.1039/c5ra20137c

It is worth mentioning that there are only a few papers[15] describing use of "grafting from" strategy for anchoring DTC to the MNP surface. RAFT/MADIX polymerization reactions were conducted to prepare polymeric shells around magnetic cores. Three different monomers were utilized to obtain homopolymeric, random and block copolymeric shells with chelating properties. Additionally, post-modification reaction – the second method for introducing chelating groups on the MNP surface – was investigated. Anchoring polymers on MNP allows fast separation of nanohybrids, good recovery after usage and also enables reapplication of the material. Since acetylacetonate based ligands are broadly used in different areas of science and industry, and recovery of its complexes is of great importance, anchoring of acetylacetone type ligands on magnetically separable solid phase seems to be very promising solution. It is worth of pointing out that up-to-date, there is only one report describing acetylacetone based polymers (obtained by non-controlled radical polymerization) and their composites (not nanohybrids) with MNP.[16]

# 2. Experimental section

## 2.1. Materials and methods

All reagents such as acetylacetone, propargyl bromide, sodium azide, 4-vinylbenzylchloride, styrene, sodium iodide, cooper(I) iodide, sodium ascorbate were purchased from Aldrich Chemical Company and used as received. Hexane, dichloromethane and ethyl acetate were purchased from Avantor Performance Materials Poland and were distilled before use. THF and acetone were purchased from Avantor Performance Materials Poland and were dried according to the standard protocols[17] before use.

## 2.2. 4-Vinylbenzylazide

A 5.1 g (78 mmol) of sodium azide and 2.28 g (6.54 mmol) of CTAB was dissolved in 430 mL of deionized water. Subsequently, 9.23 mL (65 mmol) of 4-vinylbenzylchloride were added. Reaction was stirred for 24 hours at 40 °C. After extraction (DCM) the product was purified by dry flash chromatography (hexane) and monomer was obtained as yellow oil with 95% yield.

$^1$H NMR (400 MHz, $CDCl_3$, $\delta$, ppm): 7.48 (d, 2H), 7.32 (d, 2H), 6.78 (dd, 1H, $J_1 = 10.9$ Hz, $J_2 = 17.6$ Hz), 5.83 (d, 1H, $J = 16.7$ Hz), 5.34 (d, 1H, $J = 10$ Hz), 4.35 (s, 2H); $^{13}$C NMR (100 MHz, $CDCl_3$, $\delta$, ppm): 137.5, 136.1, 134.7, 128.3, 126.5, 114.3, 54.4; FT-IR (ATR, $\nu$) cm$^{-1}$: 3088, 2928, 2931, 2094, 1242, 990, 822.

## 2.3. 3-Propargylpenta-2,4-dione

1.49 g of dried potassium carbonate (10.8 mmol) was placed in a flask and then dried acetone was added (100 mL). Simultaneously, 1 mL (9 mmol) of propargyl bromide (80% solution in toluene) and 4.4 mL (45 mmol) of acetylacetone were added. The reaction was stirred for 24 hours at 60 °C at inert atmosphere. Next, the mixture was filtrated and the solvent was removed under reduced pressure. The product was purified by dry flash chromatography (hexane : dichloromethane 7 : 3). It was obtained as yellow oil, yield 86%.

$^1$H NMR (400 MHz, $CDCl_3$, $\delta$, ppm): 3.86 (t, 1H, $J = 7.5$ Hz), 3.12 (d, 2H, $J = 2.7$ Hz), 2.70 (dd, 2H, $J_1 = 2.6$ Hz, $J_2 = 7.5$ Hz), 2.26 (s, 6H), 2.23 (s, 6H), 2.03 (t, 1H, $J = 2.7$ Hz); $^{13}$C NMR (100 MHz, $CDCl_3$, $\delta$, ppm): 202.1, 190.8, 106.4, 81.6, 80.2, 70.7, 68.6, 66.5, 29.3, 23.0, 17.3; FT-IR (ATR, $\nu$) cm$^{-1}$: 3308, 3024, 1731, 1702, 1604, 1421, 1360, 1152, 646.

## 2.4. "Click" reaction

55 mg (0.29 mmol) of cooper(I) iodide and 30 mL of dried THF were placed in a flask. Then, 507 mg (3.19 mmol) of 4-vinylbenzylazide, 400 mg (2.9 mmol) of 3-propargylpenta-2,4-dione, 1 mL (5.8 mmol) of diisopropylethylamine (DIPEA) and 50 mg (0.29 mmol) of sodium ascorbate were added. The reaction mixture was stirred at inert atmosphere at 40 °C for 24 hours. Next, the solvent was removed under reduced pressure, reaction mixture was diluted by ethyl acetate and the catalyst was filtrated on Celite. Subsequently, the mixture was washed by aq. 10% HCl and dried over anhydrous $Na_2SO_4$. The product was purified by dry flash chromatography (hexane : ethyl acetate, 8 : 2 with 1% triethylamine). The 648 mg (2.18 mmol) of white solid was obtained, 56% yield.

$^1$H NMR (400 MHz, $CD_3OD$, $\delta$, ppm): 7.68 (s, 1H), 7.28 (m, 2H), 7.22 (m, 2H), 6.71 (dd, 1H, $J_1 = 11$ Hz, $J_2 = 6.7$ Hz), 5.77 (d, 1H, $J = 17.2$ Hz), 5.50 (s, 2H), 5.24 (d, 1H, $J = 11$ Hz), 3.15 (s, 2H), 2.17 (s, 6H); $^{13}$C NMR (100 MHz, $CD_3OD$, $\delta$, ppm): 205.4, 192.7, 148.7, 146.1, 139.3, 137.4, 129.3, 127.7, 124.2, 114.9, 109.0, 67.6, 54.6, 29.9, 24.7, 23.4; FT-IR (ATR, $\nu$) cm$^{-1}$: 3119, 3072, 2995, 2926, 1699, 1629, 1511, 1315, 1046; mp: 74.7–76.0 °C; MS ($m/z$): calculated for $C_{17}H_{19}N_3O_2$ −297.36, found 297.15; EA: 69.0% C, 6.2% H, 13.7% N, 11.1% O (calculated 68.7% C, 6.4% H, 14.1% N, 10.8% O).

## 2.5. 3-(4-Vinylbenzyl)penta-2,4-dione

Into a 25 mL round bottomed flask, 1.06 g (4.3 mmol) of 4-vinylbenzyliodide was placed. Subsequently, 6 mL (58.1 mmol) of acetylacetone and 1.2 g (8.7 mmol) of dried potassium carbonate were added. Reaction was stirred for 24 hours in 50 °C, after completion of reaction (TLC) excess of acetylacetone was evaporated and 20 mL of DCM was added. Potassium carbonate was then drained and solvent was evaporated. Crude product was purified using dry flash chromatography (hexane : dichloromethane, 1 : 1). The product was obtained as yellow oil, 70% yield.

$^1$H NMR (400 MHz, $CD_3Cl$, $\delta$, ppm): 7.34 (m, 4H), 7.12 (m, 4H), 6.70 (dd, 2H, $J_1 = 10.3$ Hz, $J_2 = 17.6$ Hz), 5.72 (d, 2H, $J = 13.3$ Hz), 5.22 (d, 2H, $J = 10.4$ Hz), 4.00 (t, 1H, $J = 7.5$ Hz), 3.65 (s, 2H), 3.14 (d, 2H, $J = 7.5$ Hz), 2.13 (s, 6H), 2.08 (s, 6H); $^{13}$C NMR (100 MHz, $CD_3Cl$, $\delta$, ppm): 203.2, 191.8, 139.3, 137.6, 135.8, 128.7, 127.5, 126.5, 113.6, 113.4, 108.1, 69.8, 33.9, 32.6, 29.6, 23.3; FT-IR (ATR, $\nu$) cm$^{-1}$: 3085, 3005, 2924, 1727, 1699, 1605, 1510, 1406, 1356, 990, 907.

## 2.6. General procedure for surface initiated polymerization

Magnetic nanoparticles with dithiocarbonate groups on their surface (50 mg) were sonically dispersed in 2 mL of toluene. Then, the monomer (50 mg) and 2 mg of AIBN were added. The

 

reaction mixture was stirred for over 24 h at 80 °C. The initiator was added partially (each part was 2 mg), after 2, 6 and 16 hours of stirring. Next, the nanoparticles were separated by external magnetic field and washed at least 3 times by toluene and then by methanol. The product was dried at 60 °C overnight.

In the case of random copolymerization monomers were mixed in molar ratio 1 : 5 (bifunctional monomer : styrene).

For block copolymerization reaction styrene coated nanoparticles with 11% of polystyrene content were taken as a starting material.

### 2.7. General procedure for post modification reaction

Magnetic nanoparticles with polymeric shells (25 mg) were sonically dispersed in 1.5 mL of dried THF. Then 3-propargylpenta-2,4-dione (25 mg), 3.45 mg of cooper(I) iodide, 3.56 mg of sodium ascorbate and 63 μL of dried DIPEA were added to the magnetic nanoparticles solution. The reaction mixture was stirred at inert atmosphere at 40 °C for 4 days. Next, the nanoparticles were separated by placing in an external magnetic field and then washed by deionized water and methanol. The product was dried at 60 °C overnight.

### 2.8. General procedure for complexation reaction of lanthanides

Magnetic nanoparticles with polymeric shell (20 mg) were sonically dispersed in 2 mL of methanol. Then 2.6 μL of piperidine was added and mixture was stirred for 15 min. Afterwards 2.5 mg of lanthanide chloride was added and stirred at room temperature for 24 hours. Nanoparticles were separated by using external magnetic field, and washed by deionized water and methanol. The product was dried at 60 °C overnight.

### 2.9. Measurements

The formation of magnetic nanoparticles, particle size and morphology were confirmed by transmission electron microscopy (TEM) (Tecnai G2 X-TWIN). Samples for TEM were prepared on holey carbon cooper grids. Energy-dispersive X-ray spectroscopy (EDX – detector Ametek Octane Pro) analyses were collected from the samples imaged by SEM (TFP 2017/12 Inspect S50 FEI). Samples for SEM microscopy were prepared on aluminium tables and were covered by 4 nm Au layer (Leica ACE 200 coater) in order to improve imagining. Surface modifications were confirmed by ATR FT-IR (Nicolet 6700). Thermogravimetric analysis (TGA) was performed on a Mettler Toledo Star TGA/DSC unit. Differential scanning calorimetry (DSC) was performed on a Mettler Toledo Star DSC system. Argon was used as a purge gas (200 mL $min^{-1}$ – DSC, and 20 mL $min^{-1}$ – TGA). Samples between 2 and 5 mg were placed in aluminium pans and heated from 50 °C to 950 °C (TGA) or from 25 °C to 480 °C (DSC) with a heating rate of 10 °C $min^{-1}$. The $^{1}H$ NMR and $^{13}C$ NMR spectra were recorded on a Bruker Avance II spectrometer (400 MHz and 100 MHz respectively). The melting points were measured by Mettler Toledo MP 70 Melting Point System. Elemental analyses were performed on Elementar Vario Micro Cube, UV-Vis spectra were investigated on Jasco V-670 Spectrophotometer and luminescence analyses were done on Hitachi F7000 Fluorescence Spectrophotometer. Magnetic properties of the nanoparticles were studied using a Quantum Design MPMS 5XL SQUID-type magnetometer. Each sample was placed in a standard gelatine capsule and immobilised with varnish glue for the measurement. All the data were carefully corrected for the diamagnetic contribution of the holder.

## 3. Results and discussion

### 3.1. Synthesis of new bifunctional monomers

Three different vinyl monomers were synthesized (Fig. 1) and then used for preparation of polymeric shells on magnetic nanoparticles.

Two of them contain acetylacetonate moiety (monomer **2** and monomer **3**). The presence of azide groups on the third one (monomer **1**) allows further modification after polymerization reaction resulting in introducing of β-diketone groups onto the polymeric shell. Synthesis of monomer **2** was performed in a three-step synthetic path. Firstly, the 4-vinylbenzylazide (monomer **1**) was synthesized in the substitution reaction of 4-vinylbenzylchloride with sodium azide using standard phase transfer catalysis protocol (with CTAB as surfactant).[18] Next, acetylacetonate acetylene (**2a**) derivative was obtained in substitution reaction of acetylacetone by propargyl bromide (mole ratio 5 : 1) with potassium carbonate as base and acetone as solvent.[19] In this reaction, excess of acetylacetone was used to avoid formation of by-product – 3,3-disubstituted acetylacetone. The last step was "click" type Huisgen reaction which allows preparation of 1,2,3-triazole bifunctional derivatives (Fig. 1.2). The product of copper catalyzed Huisgen reaction should be obtained at the room temperature, unfortunately in our case stirring at room temperature even for one week was not effective. According to the structure of starting material (presence of vinyl bond sensitive for light and temperature) the reaction mixture was slightly heated and covered against sunlight. Under such conditions the desired product was obtained with several percent of yield. Furthermore, it was observed that heating of the reaction mixture till 40 °C does not cause polymerization of

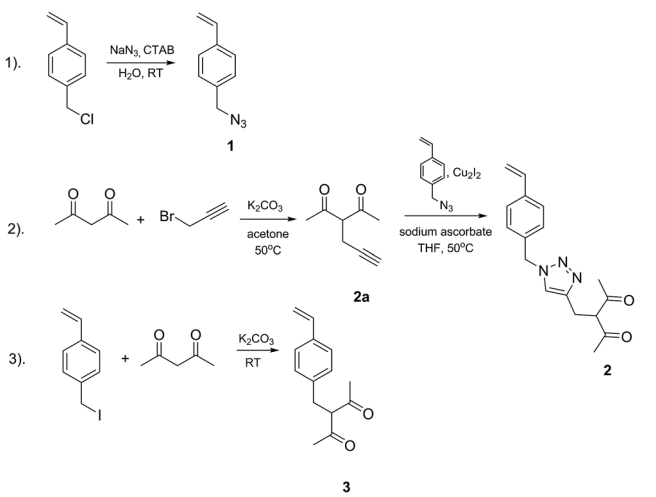


Fig. 1 Synthesis of three different vinyl monomers.

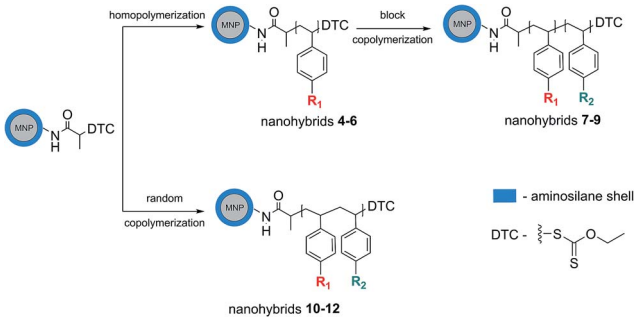


Fig. 2 Synthesis of polymeric shells (DTC – dithiocarbonate).

4-vinylbenzylazide and thus the Huisgen reaction was carried out at this temperature. After 24 hours of stirring at 40 °C the product (monomer **2**) was obtained with 75% yield. According to the literature,[20] during a cooper-catalysed Huisgen reaction only one regioisomer should be formed (1,4-substituted 1,2,3-triazole). In our case, mixture of two 1,4- and 1,5-substituted regioisomers was obtained (mole ratio 3 : 1 respectively, confirmed by NMR and HPLC). The mixture of regioisomers was purified using dry column chromatography. In further research, only 1,4-substituted regioisomer was considered (produced with 56% yield). This monomer was polymerized on the surface of dithiocarbonate-coated magnetic nanoparticles using surface initiated RAFT/MADIX polymerization technique. In order to compare the properties of the obtained polymeric shell, another two monomers known from the literature were synthesized and polymerized as well. The monomer **3** (firstly synthesized by Dow Chem. Co.[21]) was prepared *via* a new synthetic protocol, including usage of 4-vinylbenzyliodide (Fig. 1.3). Monomers **2** and **3** were prepared in the scope of investigation of influence of linkage between vinyl and acetylacetone functional groups on chelating properties of the obtained polymers.

### 3.2. Surface initiated polymerization reactions

In this research, core–shell superparamagnetic nanoparticles with iron oxide core and aminosilane shell were used.

Their synthesis, characterization and applications were described in our previous papers.[15a,22] The ethyl dithiocarbonate (DTC) was used as chain transfer agent and was covalently bonded to the surface of nanoparticles.[15a] RAFT/MADIX polymerization was employed to create polymeric shells with chelating properties.

To investigate the relation between polymeric shell structure and its chelating activity, three types of polymerization were performed on the surface of MNP: homopolymerization, block copolymerization and random copolymerization (Fig. 2).

Homopolymerization introduces the largest amount (mass ratio) of functional groups on the surface of MNP, however, the steric hindrance can reduce their availability for metal ions. For this reason, random copolymers were prepared with styrene as

Table 1 Polymeric shells anchored on MNP

| Type of polymeric shell | No. of nanohybrid | Type of monomer | | % of mass decomposition (by TGA) |
|---|---|---|---|---|
| | | $R_1$ | $R_2$ | |
| Homopolymer | **4** | $-CH_2N_3$ | — | 25 |
| | **5** | 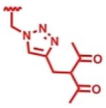 | — | 33 |
| | **6** |  | — | 34 |
| Random copolymer | **7** | –H | $-CH_2N_3$ | 31 |
| | **8** | | 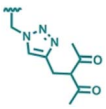 | 23.5 |
| | **9** | |  | 16.5 |
| Block copolymer | **10** | –H | $-CH_2N_3$ | 54 |
| | **11** | | 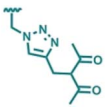 | 64 |
| | **12** | |  | 17 |

 

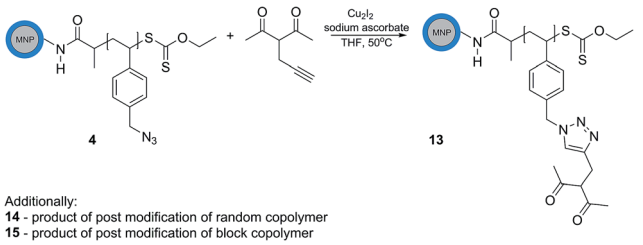


Fig. 3 Scheme of post modification reaction.

comonomer. Styrene units in the polymer chain separate large functional groups of synthesized monomers, improving availability of chelating moiety. The block copolymers were prepared in order to test if the distance between functional groups and magnetic core affects the properties of polymeric shells. In the instance of the homopolymer, the functional polymeric shell is very close to the magnetic core whereas in the case of the block copolymer, two polymeric layers were prepared one after another. As a result, MNP with inner polystyrene and external chelating shells were obtained. Additionally, polymerization of 4-vinylbenzylazide on MNP was performed. In the next step, azide groups were modified further. The influence of the method of shell preparation on its chelating properties was investigated.

All polymerization reactions were handled in the same conditions *i.e.* stirring for 24 hours at 80 °C in toluene. Initially, three different solvents were investigated: methanol, THF and toluene. The best results *i.e.* the highest thicknesses of polymeric shell (determined by TG analysis) were obtained using toluene as a solvent. AIBN was used as an initiator and it was added in three portions, at the beginning of the polymerization, after two hours and after 16 hours of stirring at inert atmosphere. All the results are presented in Table 1. Additionally, RAFT/MADIX polymerization reaction of monomer **2** in solution was performed. $T_g$ of the obtained polymer determined by the DSC method was 65 °C (see ESI†).

It can be noticed that the highest mass increase occurred in the cases of block copolymerization reactions (MNP **10**, MNP **11**). Homopolymerization reactions also gave good results. The lowest mass increase was observed in copolymerization reaction with monomer **3** as a starting material (MNP **9**). This result suggests low polymerizability of this monomer. Owing to the lowest efficiency of random copolymerization reactions, MNP with homopolymeric and block copolymeric shells were studied further.

### 3.3. Post-modification reaction

As it was mentioned above, preparation of monomer **2** was time- and cost-consuming (56% yield after separation of mixture of regioisomers) and took three steps in the synthetic path. Furthermore, despite the facility of producing monomer **3** it shows poor polymerizability in the applied conditions. For these reasons another way of introducing chelating groups on the MNP surface was applied. Azide-functionalized polymeric shells (homo- and copolymeric) were obtained (MNP **4**, **7** and **10**). Since the CuAAC (copper catalyzed azide–alkyne coupling)

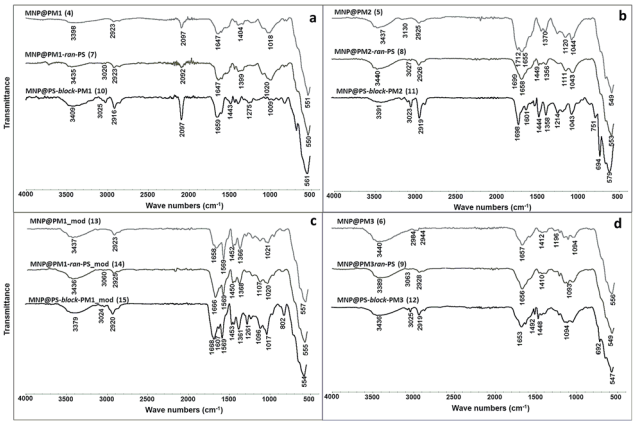


Fig. 4 ATR FT-IR spectra of polymer modified MNP.

"click" reaction was raised as the most useful and widely employed functionalization way within polymer chemistry,[23] the Huisgen "click" reaction protocol was applied to modify azide-functionalized polymeric shells. In this manner, nanoparticles were sonically dispersed in dried THF and then 3-propargylpenta-2,4-dione (**2a**), copper(I) iodide and sodium ascorbate were added (Fig. 3).

The mixture was stirred for 4 days at 40 °C. The introduction of the acetylacetone moiety was investigated by ATR FT-IR spectroscopy. Each of the polymeric nanohybrids containing azide groups were modified in this way. As a result, three different sorts of materials were obtained, *i.e.* nanoparticles covered by homopolymeric, random copolymeric and block copolymeric sells (**13**, **14** and **15** respectively). The reaction was stopped when the characteristic peak of $-N_3$ moiety at around 2000 $cm^{-1}$ disappeared. A large advantage of this process is the very fast purification of the product after the reaction (separation by external magnetic field took approx. 10 minutes). Additionally, in this case, chromatography protocol, applied for purification of monomer **2**, was omitted. Nevertheless, this process has some disadvantages. As it was mentioned before, the Huisgen reaction gives two regioisomers (1,4- and 1,5-substituted) as products and their formation in the post-modification reaction cannot be excluded. Moreover, there is no certainty that 100% of azide groups were modified due to their steric inaccessibility.

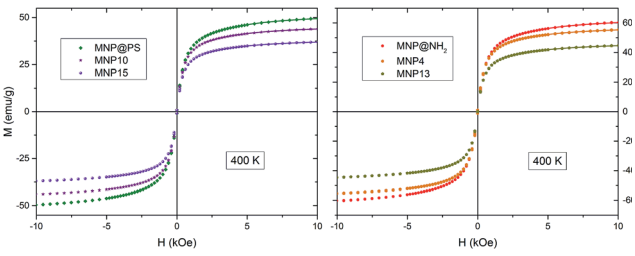


Fig. 5 Magnetisation as a function of external magnetic field measured for MNP with polystyrene shell (MNP@PS) compared with MNP **10** and **15** (left) and MNP with aminosilane shell compared with MNP **4** and **13** measured in 400 K. Solid lines represent LA fits to the data.

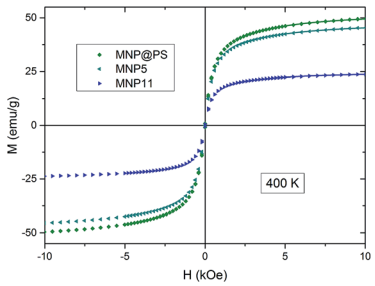


Fig. 6 Magnetisation as a function of external magnetic field measured for MNP with polystyrene shell compared with MNP **5** and **11**, at 400 K. Solid lines represent LA fits to the data.

### 3.4. Characterization of MNP with polymeric shell

Obtained polymeric nanohybrids were characterized by ATR FT-IR spectroscopy, TG analyses, DSC, TEM and SEM microscopy. Magnetic properties were also investigated.

**3.4.1. Infrared spectra.** The FT-IR spectra off all modified nanoparticles are presented in Fig. 4. In the IR spectra of MNP after polymerization and copolymerization reactions the characteristic peaks at around 560 and 1100 $cm^{-1}$ can be assigned to Fe–O and Si–O stretching bonds respectively (Si–O bonds are presented in the inorganic shell which was created by a sol–gel method with APTMS as starting material).[15,22]

Additionally, two peaks at around 2900 $cm^{-1}$ represent stretching bond of $-CH_2$ groups present in polymeric chain and the one over 3000 $cm^{-1}$ represent stretching bonds of –C–H present in aromatic rings. In the 4-vinylbenzylazide spectra of modified nanoparticles (Fig. 4a) the characteristic peaks around 2000 $cm^{-1}$, representing stretching bonds of azide group, occurred. In the spectra of MNP modified by polymerization reactions of monomer **2** (Fig. 4b) two characteristic peaks were observed. First, at around 1700 $cm^{-1}$ represents stretching of C=O group present in the acetylacetonate moiety, second at around 1650 $cm^{-1}$ corresponds to the stretching bond of the C–H group in 1,2,3-triazole ring. After a chemical modification of materials **4**, **7** and **10** characteristic peak of C=O stretching bond occurred at around 1680 $cm^{-1}$, and also, strong narrow peak at 1569 $cm^{-1}$ that can be assigned to N=N stretching bond (present in 1,2,3-triazole ring) appeared.

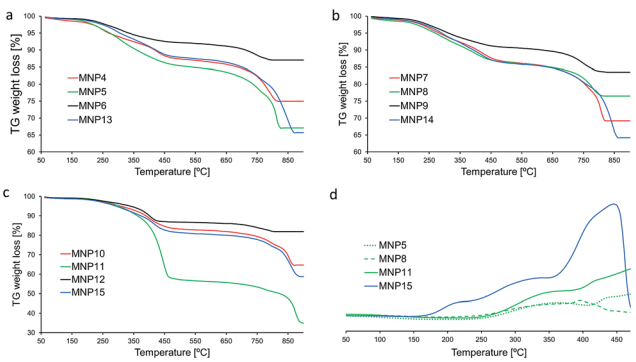


Fig. 7 TGA and DSC curves of synthesized nanohybrids.

**3.4.2. Magnetisation.** Magnetisation *versus* field curves were measured within a range of temperatures. The bare nanoparticles exhibited superparamagnetic behaviour at room temperature, however, for the rest of the samples it was necessary to increase the temperature up to the experimentally available maximum of 400 K to approach the superparamagnetic region and to obtain closing of the hysteretic loops that were still visible at 300 K. Law of approach to saturation (LA) was fitted to the data in high magnetic fields to obtain the values of the saturation magnetisation.[24]

It can be observed (Fig. 5) that introduction of new functional groups to polymeric shell using the post-modification reaction slightly reduces the value of the saturation magnetisation (*e.g.* from 68.9 to 64.3 and 52.5 emu $g^{-1}$, for MNP@$NH_2$, MNP **4** and **13**, respectively).

On the other hand, increasing of thickness of polymeric shell (creation of block copolymeric shell) causes reduction of the value of $M_S$ by over a half (for the MNP coated by PS-*block*-M2 polymeric shell (**11**) $M_S$ = 27.6 emu $g^{-1}$ – Fig. 6).

It was proven that magnetisation values barely depends on the type of monomer which creates the polymeric shell (the $M_S$ values oscillate from 45.5 – MNP **5** to 55.5 emu $g^{-1}$ – MNP **4**).

**3.4.3. Thermogravimetric analyses.** TGA studies were carried out for magnetic nanoparticles after polymerization reactions of three presented monomers (homo, random, and block polymerization), and after chemical modification of polyazides present on MNP.

Fig. 7 shows the TG curves of magnetic nanoparticles covered by: homopolymers MNP **4**, MNP **5**, MNP **6** and MNP **13** (Fig. 7a), random copolymers MNP **7**, MNP **8**, MNP **9** and MNP **14** (Fig. 7b) and block copolymers MNP **10**, MNP **11**, MNP **12** and MNP **15** (Fig. 7c). TG curve refers to the temperature-dependent mass change in percent, and DTG curve refers to the rate of mass change (see ESI†). The TGA curves show weight loss from 13 to 35% for all nanohybrids with homopolymers, 16.5–36% and 18–66% for nanoparticles covered by random polymeric and block copolymeric shells, respectively. For the block copolymerization, polystyrene nanoparticles with 11% of polystyrene weight content were used. Comparing the shell type (homopolymeric and copolymeric) and influence of the monomer type, the best polymerization results were obtained in the case of monomer **2**, whereas the lowest mass increase was achieved for monomer **3**. In the thermograms of all nanohybrids, two

Table 2 Comparison of mass decomposition during TGA analyses for nanohybrids before and after post modification

| Type of polymeric shell | Post modification | Sample | % of mass decomposition (by TGA) |
|---|---|---|---|
| Homopolymer | No | MNP **4** | 25 |
| | Yes | MNP **13** | 34 |
| Random copolymer | No | MNP **7** | 31 |
| | Yes | MNP **14** | 36 |
| Block copolymer | No | MNP **12** | 35 |
| | Yes | MNP **15** | 41.5 |

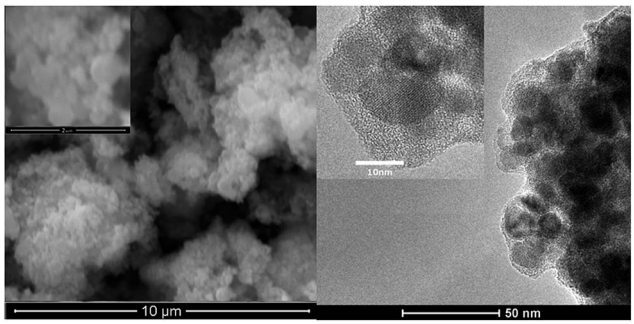


Fig. 8 SEM and TEM photographs of MNP **12** with samarium ions.

broad degradation region between 200 and 500 °C, and between 700 and 850 °C were observed (TGA/DTG curves are presented in ESI†). Typical region of decomposition of polystyrene is about 400–450 °C.[15] The changes in the degradation regions confirm modification of nanoparticles by azide and acetylacetone groups. Additionally, in the case of post-modified nanoparticles higher weight loss was observed in comparison to polyazide covered nanohybrids. It is caused by the increase of weight during "click" reaction on polyazide shells (Table 2) (Fig. 7).

In Fig. 7d, DSC curves of nanohybrids: MNP **5**, MNP **8**, MNP **11** with homopolymeric coating and after post modification of azide moiety (MNP **15**) were presented. Differences in the shape of DSC heating curves of nanoparticles confirm changes in the chemical nature of polymeric shells obtained from different monomers as well as before and after "click" reaction.

### 3.5. Polymer modified nanoparticles as magnetically separable complexing agents

For the investigation of chelating properties of MNP with polymeric shells three different lanthanide ions ($Er^{3+}$, $Sm^{3+}$, $Nd^{3+}$) were chosen (Fig. 8).

In the complexation reactions only nanoparticles with homopolymeric and block copolymeric shells were tested. Furthermore, to compare complexing properties of different kind of chelating agents towards lanthanide ions (erbium, samarium and neodymium) nanoparticles **4** and **5** were used. Simultaneously, complexation reactions with lanthanides and nanohybrids **10** were conducted in order to investigate the dependence of complexing properties on polymeric shell structure (Table 3).

The results show that azide groups (present in the homopolymeric shell of MNP **4**) have minor ability to complex lanthanide ions than MNP with block copolymeric shell with 4-vinylbenzylazide as co-monomer (MNP **10**). The latter ones show the highest amount of complexed ions (excluding erbium ion). For further tests samarium ions were chosen because of good results of complexation reaction in all cases. Subsequently, complexing properties towards samarium ion were investigated for nanohybrids **6**, **11**, **12**, **13** and **15**. The results clearly show that the amount of complexed metal heavily depends on the structure of the polymeric shell (Table 4 and Fig. 9).

Nanoparticles with block copolymeric shell complexed a greater amount of samarium ions than MNP with homopolymeric shells. Nanohybrids **13** and **15** occurred to be the least efficient chelating nanohybrids (with approx. samarium ion content 4.5 and 10% respectively).

The IR spectra of MNP after complexation reaction clearly picture structural changes. Primarily, shift of C=O stretching band towards lower wavenumbers (from 1712 to 1590 $cm^{-1}$) is observed.

Furthermore, small peak at around 1540 $cm^{-1}$ which corresponds to characteristic C=C bond in acetylacetonate complexes has occurred (Fig. 10).

TGA and DSC analyses for the MNP with lanthanide ions were performed and are presented in Fig. 11. Lower weight loss observed on the TGA curve of complexes is associated with the lanthanide residuals. The best results of complexation reaction of samarium ions were observed in the case of nanohybrids with homopolymeric shell obtained with monomer **2**. The changes derived from complexes formation were also observed on DSC heating curves. Additionally, nanoparticles covered by block copolymers with samarium ions were investigated. The results

Table 3 Content of complexed lanthanide ions calculated by SEM/EDX (values are in mass%)

| Compound\metal ion | $Er^{3+}$ | $Sm^{3+}$ | $Nd^{3+}$ |
|---|---|---|---|
| MNP@PM1 (**4**) | 10.66 ± 0.37 | 7.93 ± 0.14 | 7.37 ± 0.03 |
| MNP@PM2 (**5**) | 12.95 ± 1.06 | 10.24 ± 0.48 | 7.49 ± 0.55 |
| MNP@PS-*block*-PM1 (**10**) | 1.40 ± 0.41 | 21.03 ± 0.59 | 10.88 ± 0.83 |

Table 4 Content of samarium ions in different polymeric nanohybrids

| Nanohybrids with samarium complex | $Sm^{3+}$ [%mass][a] |
|---|---|
| MNP@PM1 (**4**) | 7.93 |
| MNP@PS-*block*-PM1 (**10**) | 21.03 |
| MNP@PM2 (**5**) | 10.24 |
| MNP@PS-*block*-PM2 (**11**) | 11.70 |
| MNP@PM3 (**6**) | 7.47 |
| MNP@PS-*block*-PM3 (**12**) | 10.58 |
| MNP@PM1_mod (**13**) | 4.51 |
| MNP@PS-*block*-PM1_mod (**15**) | 9.96 |

[a] Calculated by SEM/EDX.

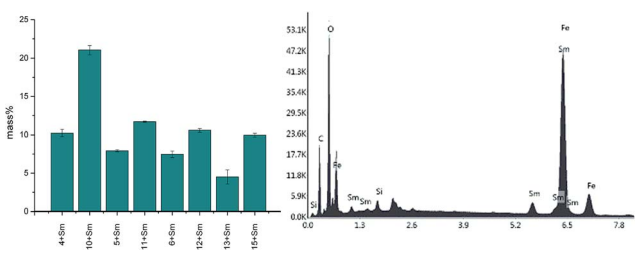


Fig. 9 Content of samarium ions in different polymeric nanohybrids (left) and an example of SEM/EDX spectra (right).

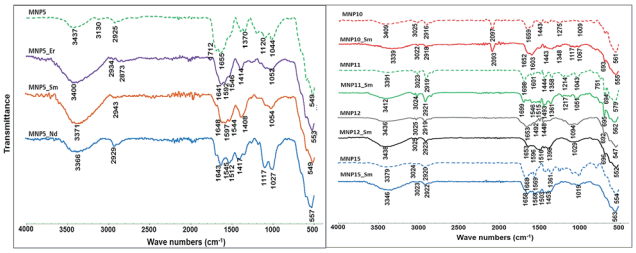


Fig. 10 ATR FT-IR spectra of MNP after reaction with lanthanides.

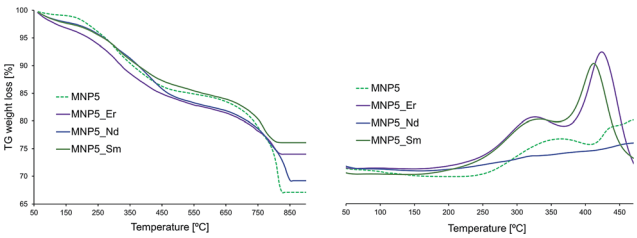


Fig. 11 TGA (left) and DCS (right) heating curves for lanthanide complexes of MNP **5**.

obtained by the DSC method are similar to the SEM/EDX investigations, the highest change in weight loss was observed in the case of MNP **10** complex with samarium (see ESI†).

It is proven that acetylacetone derivatives form complexes with lanthanides which poses luminescent properties.[25] The emission colour highly depends on type of lanthanide but is independent of the metal ion environment, *e.g.* samarium complexes emit orange light but erbium and neodymium complexes has near infrared luminescence.[4] UV-VIS and luminescence studies show slight changes that occur after complexation reaction of lanthanide ions. In the UV-Vis spectra,

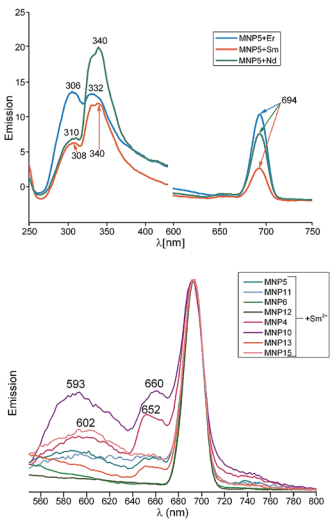


Fig. 12 Luminescence spectra of nanoparticles with homopolymeric shell consist of monomer **1** with different lanthanide ions (top) and an extended region (550–800 nm) of spectra for all samarium complexes with MNP, normalized to 1, (bottom).

mild shift of the maximum or, in some cases, extinction of the maximum is observed (see ESI†). In the luminescence spectra three emission peaks are observed. One emission peak at 694 nm, which is common for all of modified nanoparticles, corresponds to influence of exciting light with magnetic core. Two others are directly associated with the type of the complexing ion. For the neodymium ions strong peak at 340 nm is observed, and the other weaker at 310 nm. For erbium ions two peaks occur with almost the same intensity (at 306 and 332 nm).

The luminescence spectrum of samarium ions complexed with MNP **5** is similar to the neodymium one but the peak at around 340 nm is less intense. It was proven that luminescence spectra do not depend on the structure of complexing agent (they are similar for all of synthesized nanohybrids). For the rest of the investigated samarium complexes, the small broad peak around 600 nm can be observed (Fig. 12). The intensity of this peak corresponds to the amount of complexed samarium ions – the highest emission was observed for MNP **10** with $Sm^{3+}$ ions (samarium content around 21%).

## 4. Conclusions

In conclusion, new types of nanohybrids were synthesized. These nanohybrids consist of magnetic cores and polymeric shells which are covalently bonded to the surface. Therefore, they are very stable and resistant to washing off. In addition, these polymeric shells possess chelating properties. The three different chelating monomers were synthesized and used to form polymeric shells around magnetic cores by RAFT/MADIX polymerization. Also, the influence of post-modification of polymeric shell on its properties was investigated. It was proven that chemical modification of the azide groups in the polymeric shells affects their complexation properties. Unexpectedly, the best complexing properties towards lanthanide ions exhibit nanoparticles with block copolymeric shell consist of styrene and 4-vinylbenzylazide what was confirmed by SEM/EDX and luminescence spectroscopy. Despite the fact that these nanohybrids do not possess the acetylacetone moiety, they are very good complexing agents. Since complexes of azides and ion metals are heavily explosive,[26] their formation on the MNP surface appeared to be a very good alternative to the traditional methods. Furthermore, the easy method of introducing acetylacetone groups on the surface of MNP which can be further used for formation of acetylacetone-based catalysts/complexes was presented. An important feature of such catalysts/complexes is the extremely easy separation form the reaction mixture. Regardless of the way of the synthesis of polymeric shell around MNP, the magnetic measurements revealed relatively good magnetic properties for all nanohybrids.

## Acknowledgements

This work was partially financed by Polish National Science Centre, project no. NCN-2011/03/B/ST5/02691. Analyses were performed in Centre of Synthesis and Analysis BioNanoTechno of University of Bialystok. The equipment in the Centre of Synthesis and Analysis BioNanoTechno of University of

 

Bialystok was funded by EU, as a part of the Operational Program Development of Eastern Poland 2007–2013, project: POPW.01.03.00-20-034/09-00 and POPW.01.03.00-20-004/11. The authors are grateful to Dr hab. Emilia Fornal for LC-MS analysis.

## Notes and references

1 G. Pawlicki, B. Staniszewski, K. Witt, W. Urbaniak and S. Lis, *Chem. Pap.*, 2011, **65**, 221–225.
2 J. Rydberg, C. Musikas and G. R. Choppin, *Principles and Practices of Solvent Extraction*, Marcel Dekker, New York, 1992.
3 V. T. Panyushkin, A. A. Mastakov, N. N. Bukov, A. A. Nikolaenko and M. E. Sokolov, *J. Struct. Chem.*, 2004, **45**, 167–168.
4 K. Binnemans, *Chem. Rev.*, 2009, **109**, 4283–4374.
5 P. Wang, C. Fan, Y. Wang, G. Ding and P. Yuan, *Mater. Res. Bull.*, 2013, **48**, 869–877.
6 W. Liu, J. Yang, H. Xu, Y. Wang, S. Hu and C. Xue, *Adv. Powder Technol.*, 2013, **24**, 436–440.
7 H. Xie and W. Shi, *Compos. Sci. Technol.*, 2014, **93**, 90–96.
8 Y. Gao, G. Zhao, Z. Duan and Y. Ren, *Mater. Sci.-Pol.*, 2014, **32**, 66–70.
9 (*a*) X. Hu, J. Mao, Y. Sun, H. Chen and H. Li, *Catal. Commun.*, 2009, **10**, 1908–1912; (*b*) V. G. Gnanasoundari and K. Natarajan, *Transition Met. Chem.*, 2005, **30**, 433–438.
10 (*a*) F. D. Lewis and G. D. Salvi, *Inorg. Chem.*, 1995, **34**, 3182–3189; (*b*) W. Wang and L. Zhang, *Res. Chem. Intermed.*, 2014, **40**, 3109–3118.
11 V. Manivannan, J. T. Hoffman, V. L. Dimayuga, T. Dwight and C. J. Carrano, *Inorg. Chim. Acta*, 2007, **360**, 529–534.
12 Y. Ishii, S. Sakaguchi and T. Iwahama, *Adv. Synth. Catal.*, 2001, **343**, 393–427.
13 S. Perrier and P. Takolpuckdee, *J. Polym. Sci., Part A: Polym. Chem.*, 2005, **43**, 5347–5393.
14 M. Destarac, *Macromol. React. Eng.*, 2010, **4**, 165–179.
15 (*a*) A. Z. Wilczewska and K. H. Markiewicz, *Macromol. Chem. Phys.*, 2014, **215**, 190–197; (*b*) L. Wang, M. Cole, J. Li, Y. Zheng, Y. P. Chen, K. P. Miller, A. W. Decho and B. C. Benicewicz, *Polym. Chem.*, 2014, **6**, 248–255; (*c*) D. Hua, J. Tang, L. Dai, Y. Pu, X. Cao and X. Zhu, *J. Nanosci. Nanotechnol.*, 2009, **9**, 6681–6687; (*d*) G. Huang, Z. Sun, H. Qin, L. Zhao, Z. Xiong, X. Peng, J. Ou and H. Zou, *Analyst*, 2014, **139**, 2199–2206; (*e*) Y. He, Y. Huang, Y. Jin, X. Liu, G. Liu and R. Zhao, *ACS Appl. Mater. Interfaces*, 2014, **6**, 9634–9642.
16 D. Saberi, S. Mahdudi, S. Cheraghi and A. Heydari, *J. Organomet. Chem.*, 2014, **772–773**, 222–228.
17 W. L. F. Armarego and C. L. L. Chai, *Purification of laboratory chemicals*, Butterworth-Heinemann, Amsterdam, Boston, 5th edn, 2003.
18 M. Makosza, *Pure Appl. Chem.*, 2000, **72**, 1399–1403.
19 J. A. Lenhart, X. Ling, R. Gandhi, T. L. Guo, P. M. Gerk, D. H. Brunzell and S. Zhang, *J. Med. Chem.*, 2010, **53**, 6198–6209.
20 B. Dervaux and F. E. Du Prez, *Chem. Sci.*, 2012, **3**, 959–966.
21 R. C. Solvish, *US Pat.*, US3006895A, October 31, 1961.
22 (*a*) A. Z. Wilczewska and I. Misztalewska, *Organometallics*, 2014, **33**, 5203–5208; (*b*) K. Niemirowicz, I. Swiecicka, A. Z. Wilczewska, K. H. Markiewicz, U. Surel, A. Kułakowska, Z. Namiot, B. Szynaka, R. Bucki and H. Car, *Colloids Surf., B*, 2015, **131**, 29–38.
23 M. Meldal, *Macromol. Rapid Commun.*, 2008, **29**, 1016–1051.
24 V. A. Ignatchenko, R. S. Iskhakov and G. V. Popov, *Soviet Physics – JETP*, 1982, **55**, 878–886.
25 K. Binnemans, in *Handbook on the Physics and Chemistry of Rare Earths*, Elsevier, 2005, vol. 35, pp. 107–272.
26 H.-C. Wang, M. Xue, Q. Guo, J.-P. Zhao, F.-C. Liu and J. Ribas, *J. Solid State Chem.*, 2012, **187**, 143–148.